

## Article

# Genetic Diversity of Two Globally Invasive Snails in Asia and Americas in Relation with Agricultural Habitats and Climate Factors

Benliang Zhao <sup>1,2</sup>, Mingzhu Luo <sup>1</sup>, Jiaen Zhang <sup>1,2,3,\*</sup>, Yiliang Liu <sup>1</sup>, Zhixin Deng <sup>1</sup>  and Xin Gong <sup>1</sup>

<sup>1</sup> Guangdong Provincial Key Laboratory of Eco-Circular Agriculture, South China Agricultural University, Guangzhou 510642, China

<sup>2</sup> Key Laboratory of Agro-Environment in the Tropics, Ministry of Agriculture and Rural Affairs, Guangzhou 510642, China

<sup>3</sup> Guangdong Laboratory for Lingnan Modern Agriculture, Guangzhou 510642, China

\* Correspondence: jeanzh@scau.edu.cn; Tel./Fax: +86-020-85285505

**Abstract:** The successful establishment of invasive populations is closely linked to environmental factors. It is unclear whether coexisting species in the native area follow the same genetic pattern in the invaded continents under the local climate factors. Two coexisting morphologically similar snails (*Pomacea canaliculata* and *P. maculata*), native to tropical and sub-tropical South America, have become invasive species for agriculture production and wetland conservation across five continents over 40 years. We analyzed the correlation between the genetic diversity of the two snails and the climate factors or habitat changes. Based on the 962 sequences from the invaded continents and South America, the nucleotide diversity in the agricultural habitat was low for *P. canaliculata*, whereas it was high for *P. maculata*, compared with that in the non-agricultural habitat. The two snails showed a divided population structure among the five continents. The *P. canaliculata* population in the invaded continents has remained stable, whereas the *P. maculata* population expanded suddenly. Seven main haplotype networks and two ancestral haplotypes (Pc3, Pm1) were found in the *P. canaliculata* and *P. maculata* populations. The haplotypes of the two snails were related to local climate factors. The overall fixation index of *P. canaliculata* and *P. maculata* was 0.2657 and 0.3097 between the invaded continents and South America. The population expansion of the two snails fitted the isolation-by-distance model. We discovered nine new sequences from the sampling locations. Overall, the genetic diversity and genetic differentiation of the two invasive snails were closely related to geographic separation, agricultural habitat, and climate factors.



**Citation:** Zhao, B.; Luo, M.; Zhang, J.; Liu, Y.; Deng, Z.; Gong, X. Genetic Diversity of Two Globally Invasive Snails in Asia and Americas in Relation with Agricultural Habitats and Climate Factors. *Diversity* **2022**, *14*, 1069. <https://doi.org/10.3390/d14121069>

Academic Editor: Michel Baguette

Received: 19 October 2022

Accepted: 23 November 2022

Published: 4 December 2022

**Publisher's Note:** MDPI stays neutral with regard to jurisdictional claims in published maps and institutional affiliations.



**Copyright:** © 2022 by the authors. Licensee MDPI, Basel, Switzerland. This article is an open access article distributed under the terms and conditions of the Creative Commons Attribution (CC BY) license (<https://creativecommons.org/licenses/by/4.0/>).

**Keywords:** global distribution; *Pomacea* sp.; agricultural management; climate factor; genetic differentiation

## 1. Introduction

Frequent anthropogenic activity provides convenient pathways for the migration of exotic species globally by weakening the geographic barriers of isolated habitats [1]. Invasive species have become one of the primary threats to worldwide biodiversity, consistently disrupting the global ecosystem [2]. The aquatic ecosystem has suffered much from the introduced invertebrates in respect of extinctions of native fauna, changes in habitat quality, and weakening of ecosystem services [3,4]. Two coexisting gastropods indigenous to tropical and sub-tropical South America, *Pomacea canaliculata* (Lamarck, 1822) and *Pomacea maculata* Perry, 1810 (synonym: *P. insularum* d'Orbigny, 1835), have succeeded in colonizing new habitats worldwide as invasive species [5]. Apple snails such as *P. canaliculata* and *P. maculata* have spread quickly between continents over several decades after being introduced in Asia through the food and aquarium trade during the 1980s [6,7]. The Invasive Species Specialist Group has listed *P. canaliculata* as one of the world's 100 worst invasive species [8]. In wetland agriculture, the apple snails attack the seedlings and other flooded crops, and the

estimated economic loss has reached billions of dollars [9]. In natural wetlands, the apple snails have become pests as they can change the structure of the macrophyte community and disrupt ecosystem services [10]. Moreover, the apple snails act as a vital intermediate host of *Angiostrongylus cantonensis*, a nematode that threatens human health [11].

The apple snails exhibit a series of typical characteristics of r-strategist species, such as rapid growth, high reproduction, a voracious appetite, and broad physiological tolerance [5]. The two snails were found to live in a similar habitat, and their identification is extremely challenging due to the subtle external morphological traits, including shell color, shell width, tissue pigmentation, and aperture height [12–14]. Invasive populations always experience genetic limitations from founder effect and bottleneck effects [15,16]. However, multiple introductions of apple snails increase genetic diversity and facilitate the population establishment in invaded areas [15]. Recently, a new species of apple snail (*Pomacea occulta*) was identified in China in 2019, suggesting a potential evolution during the invasion of the apple snails [17]. Considering the multiple introductions, genetic evolution, adaptive behaviors, and physiological traits of the two snails, the difference in invasion pattern has posed a significant challenge to current management.

These kinds of apple snails have successfully colonized diverse habitats in tropical and sub-tropical areas in Asia, Europe, South America, North America, and Oceania [6,12]. To control the apple snails in the agricultural habitat, agricultural management methods, including molluscicides application, certain fertilizer applications (e.g., calcium cyanamide, urea), duck herding, water depth lowering, seedlings stage adjustment, and crop rotation, have also been extensively used in practice [7]. Anthropogenic activity in agriculture has inevitably influenced the populations of the two invasive snails, whereas this is relatively rare in the natural wetland [7,18]. Meanwhile, the invasion of apple snails is also restricted by the climatic characteristics in the colonized areas [19]. Invasive species need to overcome the climate obstacle before establishing a stable population and the survived individuals can tolerate the local climate in the new habitat [19,20]. Multiple introductions provided an advantage for *P. canaliculata* and *P. maculata* to sustain their invasion at the early stage. However, as the further introductions of the two snails have been prohibited due to their huge damage to agriculture and wetlands [12,15,21,22], the local climate and agricultural management have influenced the survivals of these two invasive snails after multiple introductions. However, for a long time since the two invasive freshwater snails expanded across the globe, there have been few detailed analyses of the correlation between genetic diversity, agricultural management, and climate factors.

The cytochrome oxidase subunit I (COI) sequences have provided an efficient way to identify *Pomacea* species. COI analysis has been widely used in field investigations and lab-reared conditions of the two snails, as well as in cold tolerance under the scenario of species hybridization of the two snails [20,22,23].

To understand the relationship between the genetic diversity of the two invasive snails, agricultural management, and climate factors, we retrieved the COI gene of the two apple snails from samples collected from 15 locations in China and the published COI sequences of *P. canaliculata* and *P. maculata* worldwide. After combing the geographic position, climate factors, and habitat descriptions of the sequences, we constructed a dataset composed of verified COI sequences (730 for *P. canaliculata*, 232 for *P. maculata*) in Asia, Europe, South America, North America, and Oceania. We posed the following questions: (1) Have the agricultural measures affected the genetic diversity of the two invasive snails? (2) Have the two invasive snails acclimated to the local climate factors in their invaded habitats? (3) Have the two morphologically similar snails had a close genetic pattern during global invasion? Addressing such questions aims to broaden the understanding of the invasion state of these morphologically similar invasive snails and also provide better suggestions for the prediction of their expansion and related management.

## 2. Materials and Methods

### 2.1. Sample Collection, Sequencing and Dataset Construction

We collected snails from 15 locations in southern China and stored them in an ultra-low temperature refrigerator ( $-80\text{ }^{\circ}\text{C}$ ) from 2010 to 2018. The sampling locations have differential climate traits (Supplementary Materials Table S1). Five individuals at each site were randomly selected for analysis. Total genomic DNA was extracted from the foot tissue of the frozen snails using DNA Genomic Extraction Kits (AxyPrep). The region of the COI gene was amplified by polymerase chain reaction (PCR) using the universal metazoan primers (LCO1490 and HCO2198) [24]. A volume of  $50\text{ }\mu\text{L}$  was used in the PCR reaction system, composed of  $10\times$  PCR Buffer,  $2.5\text{ mM}$  dNTPs,  $10\text{ }\mu\text{M}$  each of forward and reverse primers,  $5\text{ U}$  of Platinum<sup>TM</sup> Taq DNA polymerase (Invitrogen), and  $50\text{ ng}$  template DNA. PCR cycling conditions were  $94\text{ }^{\circ}\text{C}$  for  $120\text{ s}$ ,  $35$  cycles of  $94\text{ }^{\circ}\text{C}$  for  $30\text{ s}$ ,  $55\text{ }^{\circ}\text{C}$  for  $30\text{ s}$ , and  $72\text{ }^{\circ}\text{C}$  for  $60\text{ s}$ , followed by a final extension at  $72\text{ }^{\circ}\text{C}$  for  $300\text{ s}$  with a termination step at  $4\text{ }^{\circ}\text{C}$ . All PCR products were visualized by running products on a  $1.5\%$  agarose gel containing ethidium bromide with a  $100\text{ bp}$  ladder. The purified PCR product was sequenced using an AB-3730xl (USA).

Nucleotide sequences obtained in the study were assembled and edited using BioEdit [7.2.6.1] [25]. The resultant COI mtDNA sequences were submitted to GenBank (Accession No. MT246787-MT246854; MT246779-MT246784). We retrieved 74 sequences from all individuals except one individual from the 15 locations. No base insertions, deletions, or stop codons were determined in the recovered COI sequences. Meanwhile, we obtained the COI gene sequences of *P. canaliculata* and *P. maculata* from the GenBank database based on the following criteria: (1) Considering the synonyms between *P. maculata* and *P. insularum*, the sequences of *P. insularum* were included in the analysis of *P. maculata*. (2) The sequences used in the data had a length of over  $600\text{ bp}$  and contained no ambiguous characters. (3) The sequences were supported with geographic information. (4) The climate information consisting of temperature, precipitation, and altitude was obtained from the National Centers for Environmental Information (<https://www.ncei.noaa.gov/>) accessed on 1 October 2020 (Table 1; Supplementary Materials Figures S1–S3). The climate factors were related to the sequences corresponding to the samplings from 1980 to 2019 based on the published locations of apple snails (Supplementary Materials Table S2).

**Table 1.** The climate indicators retrieved from climate stations around the sampling locations.

Climate Factors	Indicators
Temperature	Avg. temp. (Dec–Feb) ( $^{\circ}\text{C}$ ), Avg. temp. (Mar–May) ( $^{\circ}\text{C}$ ), Avg. temp. (Jun–Aug) ( $^{\circ}\text{C}$ ), Avg. temp. (Sep–Nov) ( $^{\circ}\text{C}$ ), Avg. min. temp ( $^{\circ}\text{C}$ ), Avg. max. temp. ( $^{\circ}\text{C}$ ), Avg. temp. ( $^{\circ}\text{C}$ ), Avg. dew temp. ( $^{\circ}\text{C}$ ), Extreme lowest temp. ( $^{\circ}\text{C}$ ), Extreme highest temp. ( $^{\circ}\text{C}$ ), Days of avg. temp. $\leq 0\text{ }^{\circ}\text{C}$ (days), Days of avg. temp. $\geq 18\text{ }^{\circ}\text{C}$ (days), Days of avg. temp. $\geq 35\text{ }^{\circ}\text{C}$ (days), Days of min. temp. $\leq 0\text{ }^{\circ}\text{C}$ (days), Days of max. temp. $\geq 35\text{ }^{\circ}\text{C}$ (days)
Precipitation	Total precipitation (mm), Precipitation (Dec–Feb) (mm), Precipitation (Mar–May) (mm), Precipitation (Jun–Aug) (mm), Precipitation (Sep–Nov) (mm), Max. single-day precipitation (mm), Precipitation days (days)
Altitude	Altitude above sea level (m)

Our data contained a total of 962 sequences, which consisted of the 74 COI sequences of *P. canaliculata* and *P. maculata* obtained from the sampling positions and 888 COI sequences retrieved from GenBank and previous studies [12,13,22,23,26–40] (Supplementary Materials Table S3). The *P. canaliculata* data include 730 sequences from the invaded continents (Asia, North America, Oceania) and the native continent (South America). The *P. maculata* data include 232 sequences from the invaded continents (Asia, Europe, North America, Oceania) and the native continent (South America). The geographic positions of the sequences were

retrieved from the record or inferred from the location description in the references, which was further used to classify the sequences in the continents.

## 2.2. Analysis of Genetic Differentiation

Multiple alignments of sequences were conducted in MEGA [X] (Philadelphia, USA) using the MUSCLE algorithm [41,42]. The nucleotide composition, transition/transversion rate, singleton sites, and parsimony information sites of COI sequences of *P. canaliculata* and *P. maculata* in the invaded and native areas were analyzed in MEGA X [42]. The haplotype diversity, nucleotide diversity, mean nucleotide differences, and Tajima's D and Fu's Fs statistics with 1000 permutations were calculated using DNASP [6.0] [43] to balance the sequence size. The demographic expansion was analyzed using the sum of squared deviations (SSD) and the raggedness index (Rg) between the observed and the expected mismatch in Arlequin [3.5] under the sudden expansion model [44].

The nucleotide diversity, haplotype diversity, and 23 climate indicators were analyzed altogether through correlation analysis using the R packages 'stats' [45]. The sequences of *P. canaliculata* and *P. maculata* from Asia, Europe, North America, Oceania and South America and the corresponding 23 climate indicators for each sequence were bootstrapped (100 times) to construct a compound dataset to balance the sequence size, which was composed of 96,200 sequences supported by local climate information and then calculated for nucleotide and haplotype diversity using the R packages 'pegas' [46]. The sequences with a habitat description were used to analyze the change in genetic diversity in different habitats (Supplementary Materials Table S4). The agricultural habitat included paddy field, banana field, and taro patch, while the non-agricultural habitat consisted of natural wetland, lake, river, stream, reservoir, bayou, channel, catchment, and water pathway. The nucleotide diversity and haplotype diversity of *P. canaliculata* and *P. maculata* were analyzed between the agricultural habitat and the non-agricultural habitat through the bootstrap dataset. Bartlett and Shapiro tests were performed using the R package 'stats' before analysis [45]. The non-parametric statistical method of the Wilcoxon test was used to analyze the significance of nucleotide diversity and haplotype diversity between different habitats using the R package 'stats' [45].

Haplotype identification was carried out in DNASP [6.0], which was further used in the construction of a minimum spanning haplotype network in order to study the relationships among haplotypes of *P. canaliculata* and *P. maculata* using PopArt [1.7] [43,47]. The resultant haplotypes of *P. canaliculata* and *P. maculata* were grouped based on the mutation steps among them and then mapped to sampling locations using the R packages 'ggplot2', 'scatterpie', and 'mapproj' [48–50]. The haplotype distribution of *P. canaliculata* and *P. maculata* in the five continental populations and climate factors were analyzed through Redundancy analysis (RDA) using the R packages 'vegan', 'ggplot2', and 'ggrepel' [48,51,52].

The genetic differentiation was determined based on an analysis of molecular variance (AMOVA) using Arlequin [3.5] [43]. We used a pairwise genetic differentiation index (F<sub>ST</sub>) to evaluate the population differentiation between the invaded and native areas. The genetic structure was analyzed in three hierarchical levels: regions (Asia, Europe, North America, Oceania, and South America), populations within regions (Argentina, Brazil, Chile, China, Indonesia, Japan, Malaysia, Philippines, Spain, Thailand, United States, and Uruguay) and individuals within populations. The analogs of the F-statistics (F<sub>st</sub>, F<sub>ct</sub>, F<sub>sc</sub>) based on genetic distance were calculated to estimate the population differentiation. The pairwise F<sub>ST</sub> was calculated based on the Tamura–Nei (TN93) model in Arlequin [3.5], determined using SMS [53]. The significance level test was performed using 1000 permutations of each pairwise comparison. The correlation between geographic and genetic distances was tested with a Mantel test using the R packages 'vegan' [51].

### 3. Results

#### 3.1. Distribution and Divergence of Sequences

Based on the reported sequences, the nucleotide diversity of *P. maculata* (0–0.0320) in the invaded continents was 60% lower than that in South America, while nucleotide diversity of *P. canaliculata* (0–0.0284) was close to that in South America (Table 2). The haplotype diversity of *P. canaliculata* and *P. maculata* was, respectively, 30% and 39% lower in the invaded continents than that in South America. The mean pairwise nucleotide differences of sequences for *P. canaliculata* and *P. maculata* decreased by 98% and 47% in North America compared with those in Asia among the invaded continents. The AT-biased sequences were observed for the *P. canaliculata* and *P. maculata* (Supplementary Materials Table S5). The mean transition/transversion bias (R) value and the R value in the third codon position of the *P. canaliculata* sequences were 1.55 and 1.64 times in the invaded continents as high as those in South America. The number of variable sites, parsimony-informative sites, and singleton sites of *P. maculata* sequences decreased respectively by 11%, 27%, and 4% in the invaded continents compared with South America.

**Table 2.** Genetic diversity of *P. canaliculata* and *P. maculata*.

Regions	Sequence Number	Nucleotide Diversity	Mean Pairwise Differences	Haplotype Diversity
<i>P. canaliculata</i> in the invaded continents				
Asia	670	0.026 ± 0.013	14.829 ± 6.643	0.656 ± 0.012
North America	15	0.000 ± 0.000	0.248 ± 0.297	0.248 ± 0.131
Oceania	7	0.000 ± 0.000	0.000 ± 0.000	0.000 ± 0.000
Total	692	0.026 ± 0.013	14.902 ± 6.674	0.656 ± 0.012
<i>P. canaliculata</i> in the native area				
South America	38	0.024 ± 0.003	14.001 ± 6.423	0.933 ± 0.029
<i>P. maculata</i> in the invaded continents				
Asia	91	0.011 ± 0.003	6.722 ± 3.199	0.339 ± 0.065
Europe	8	0.000 ± 0.000	0.000 ± 0.000	0.000 ± 0.000
North America	63	0.006 ± 0.001	3.589 ± 1.847	0.699 ± 0.025
Oceania	1	0.000 ± 0.000	0.000 ± 0.000	0.000 ± 0.000
Total	163	0.012 ± 0.002	6.820 ± 2.612	0.600 ± 0.037
<i>P. maculata</i> in the native area				
South America	69	0.030 ± 0.003	17.443 ± 7.845	0.979 ± 0.006

Note: The data represent the mean ± standard deviation.

#### 3.2. Correlation Analysis, Neutrality Test and Mismatch Analysis

The nucleotide diversity of *P. maculata* in the invaded continents was mostly negatively related to temperature-derived factors and altitude (Days of avg. temp. ≤ 0 °C, Days of min. temp. ≤ 0 °C, Extreme highest temp. (°C), Altitude above sea level (m)) (Figure 1). A positive correlation was observed between the nucleotide diversity of *P. canaliculata* in the invaded continents and precipitation- and temperature-derived variables (Total precipitation, Precipitation (Mar–May, Jun–Aug, Sep–Nov), Max. single-day precipitation, Avg. temp. Jun–Aug, Avg. dew temp., Extreme highest temp., Days of avg. temp. ≤ 0 °C, Days of avg. temp. ≥ 35 °C, Days of min. temp. ≤ 0 °C, Days of max. temp. ≥ 35 °C, and Precipitation days).

The haplotype diversity of *P. maculata* in the invaded continents was positively related to climate-derived factors, except for three temperature-derived factors and altitude (Days of min. temp. ≤ 0 °C, Extreme highest temp., Days of avg. temp. ≤ 0 °C, and Altitude above sea level). The haplotype diversity of *P. canaliculata* in the invaded continents was positively related to precipitation-derived factors (Precipitation (Mar–May, Jun–Aug, and Sep–Nov), Max. single-day precipitation, Precipitation days, and Total precipitation), and temperature-derived factors (Days of avg. temp. (≤0 °C, ≥35 °C), Days of min. temp. ≤ 0 °C, Days of max. temp. ≥ 35 °C, Extreme highest temp., and Avg. dew temp.).

‘Days of avg. temp.  $\geq 35\text{ }^{\circ}\text{C}$ ’ was significantly correlated with both the nucleotide and haplotype diversity of the two snails in the invaded continents.

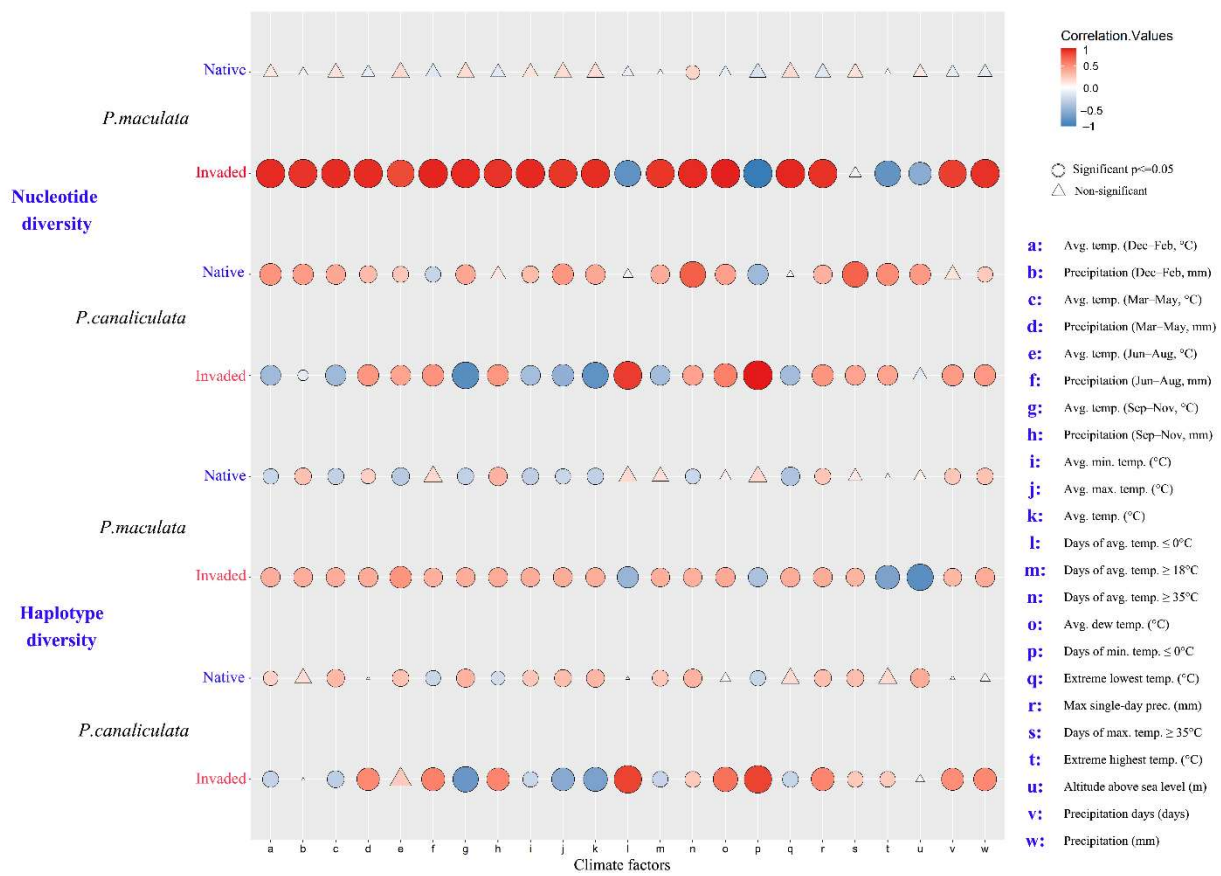


**Figure 1.** Relationship between nucleotide diversity, haplotype diversity of *Pomacea canaliculata*, *Pomacea maculata* and climate factors.

The nucleotide diversity and the haplotype diversity of *P. canaliculata* and *P. maculata* were both significantly different between the agricultural and the non-agricultural habitat ( $p < 0.001$ ) (Figure 2). The nucleotide diversity of *P. canaliculata* in the agricultural habitat was significantly lower than in the non-agricultural habitat, while the haplotype diversity of *P. canaliculata* in the agricultural habitat was significantly higher than in the non-agricultural habitat. As for *P. maculata*, the opposite trend occurred between agricultural and non-agricultural habitats.

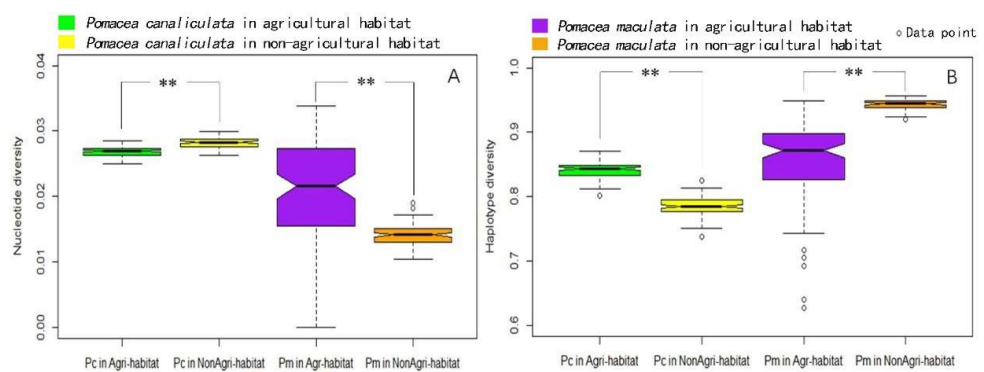


**Figure 2.** Nucleotide (A) and haplotype diversity (B) of *Pomacea canaliculata* (Pc) and *Pomacea maculata* (Pm) in agricultural and non-agricultural habitats. \*\* indicates significant differences ( $p < 0.01$ ) between the two groups.

Non-significant Tajima's D values and Fu's Fs values were obtained for the populations of the two invasive snails in the invaded continents and South America (Table 3). Based on the sum of squared deviations (SSD) and raggedness index (Rg), the demographic expansion of the *P. canaliculata* population in the invaded continents was not supported statistically (SSD = 0.236,  $p = 0.001$ ; Rg = 0.378,  $p = 0.015$ ). The value of SSD was significant for the *P. canaliculata* population in South America, while the Rg value was non-significant. A scenario of stable population demographics existed in *P. canaliculata* in the invaded continents and South America, consistent with the multimodal patterns with high Rg values in the mismatch distribution (Supplementary Materials Figure S4) after multiple introductions. However, demographic expansion was observed for the *P. maculata* population in the invaded continents (SSD = 0.131,  $p = 0.062$ ; Rg = 0.268;  $p = 0.078$ ) and South America (SSD = 0.006,  $p = 0.386$ ; Rg = 0.004;  $p = 0.783$ ) according to the mismatch distribution analysis.

**Table 3.** Neutrality and demographic expansion of *P. canaliculata* and *P. maculata*.

Species	Regions	Tajima's D	Fu's Fs	SSD	Rg
<i>P. canaliculata</i>	Invaded	0.171 (0.640)	6.496 (0.839)	0.236 (0.001)	0.378 (0.015)
	Native	−0.011 (0.585)	−1.622 (0.313)	0.043 (0.039)	0.020 (0.317)
<i>P. maculata</i>	Invaded	−0.734 (0.240)	−5.694 (0.929)	0.131 (0.062)	0.268 (0.078)
	Native	−0.841 (0.236)	−4.181 (0.166)	0.006 (0.386)	0.004 (0.783)

SSD: sum of squared deviations between the observed and the expected mismatch; Rg: Raggedness statistic; significant level at  $p < 0.05$  between parentheses.

### 3.3. Haplotype and RDA Analysis of *P. canaliculata* and *P. maculata*

We discovered seven new *P. canaliculata* haplotypes (Pc52-58; MT246812, MT246813, MT246816-MT246819, and MT246828) and two new *P. maculata* haplotypes (Pm46 and Pm47; MT246783, and MT246784) in Nanning, Sanya, Nankang and Zhangzhou, China. According to the selected sequences, there were 58 haplotypes (Pc1-58) for *P. canaliculata* and 47 haplotypes (Pm1-47) for *P. maculata* (Supplementary Materials Table S6). The number of haplotype types in *P. canaliculata* and *P. maculata* was 40 and 13 in the invaded continents, with 21 and 37 in South America, respectively.

There were four haplotypes networks in the *P. canaliculata* populations based on the mutation steps  $\leq 4$ , whereas there were three networks in the *P. maculata* populations based on the mutation steps  $\leq 6$  (Figure 3). New haplotypes of Pc55 and Pc58 in the sampling locations were not included in the above networks. The most probable ancestral haplotype Pc3 in Network I has a star-shaped topology connected to a high ratio of singletons (Figure 3; Supplementary Materials Table S6). Pc56 (MT246818) evolved to a necessary haplotype between Networks I and III. Pc6 in Asia was the most abundant haplotype in number (301/730). The probable ancestral haplotype Pm1 existed in South America, Asia, Oceania, Europe, and North America (Figure 3; Supplementary Materials Table S6). Pm7 was critical in mutation as it displayed a star-like topology with a high ratio of singletons. Both *P. canaliculata* Network I and *P. maculata* Network I dominated in the invaded continents and South America (Figure 4). *P. canaliculata* Network III and *P. maculata* Network III only existed in Asia. The frequency of *P. canaliculata* Network II in Asia was 8.1 times higher than that in South America.

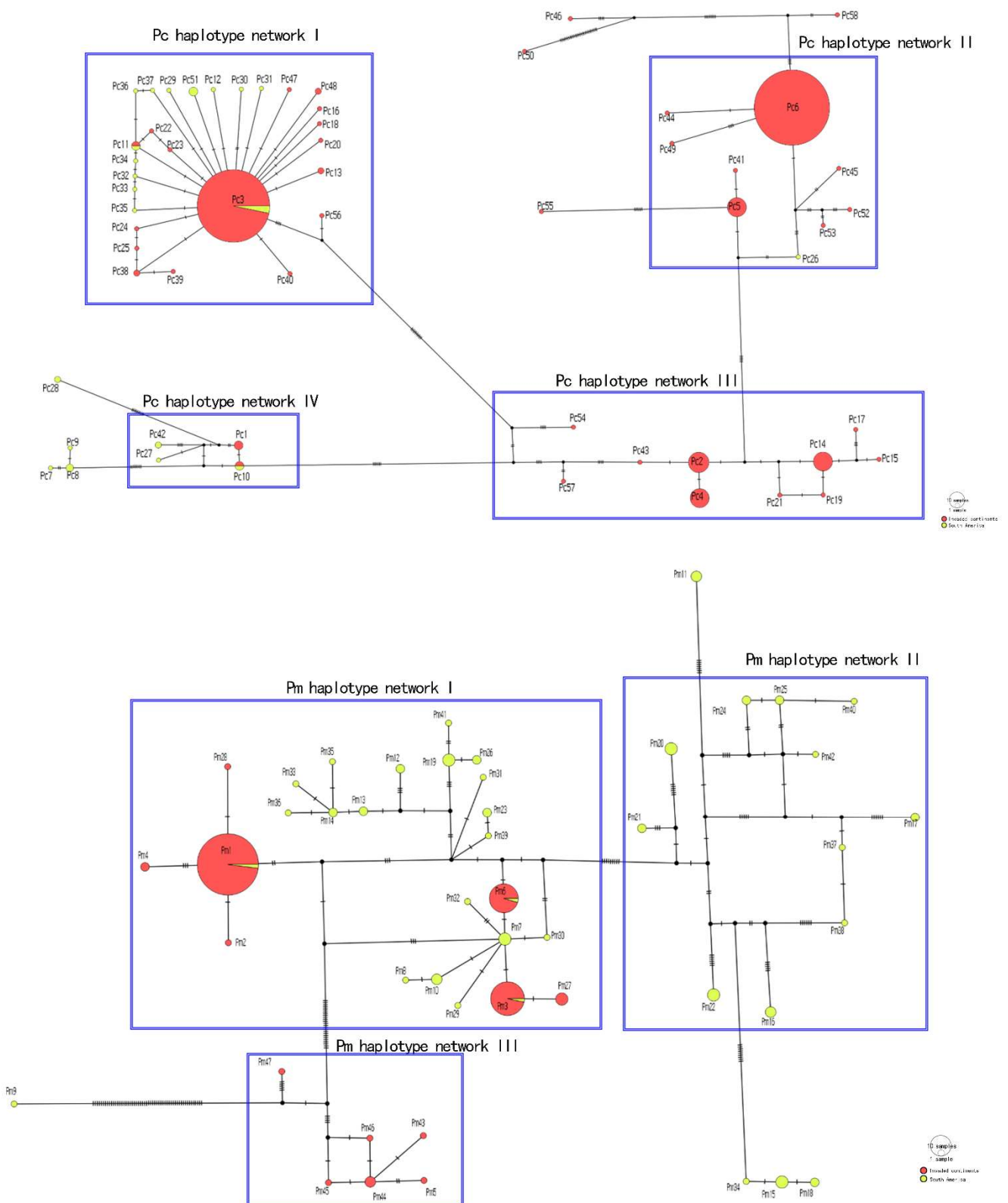


**Figure 3.** Haplotype network of *Pomacea canaliculata* (Pc) and *Pomacea maculata* (Pm) in invaded continents and South America.

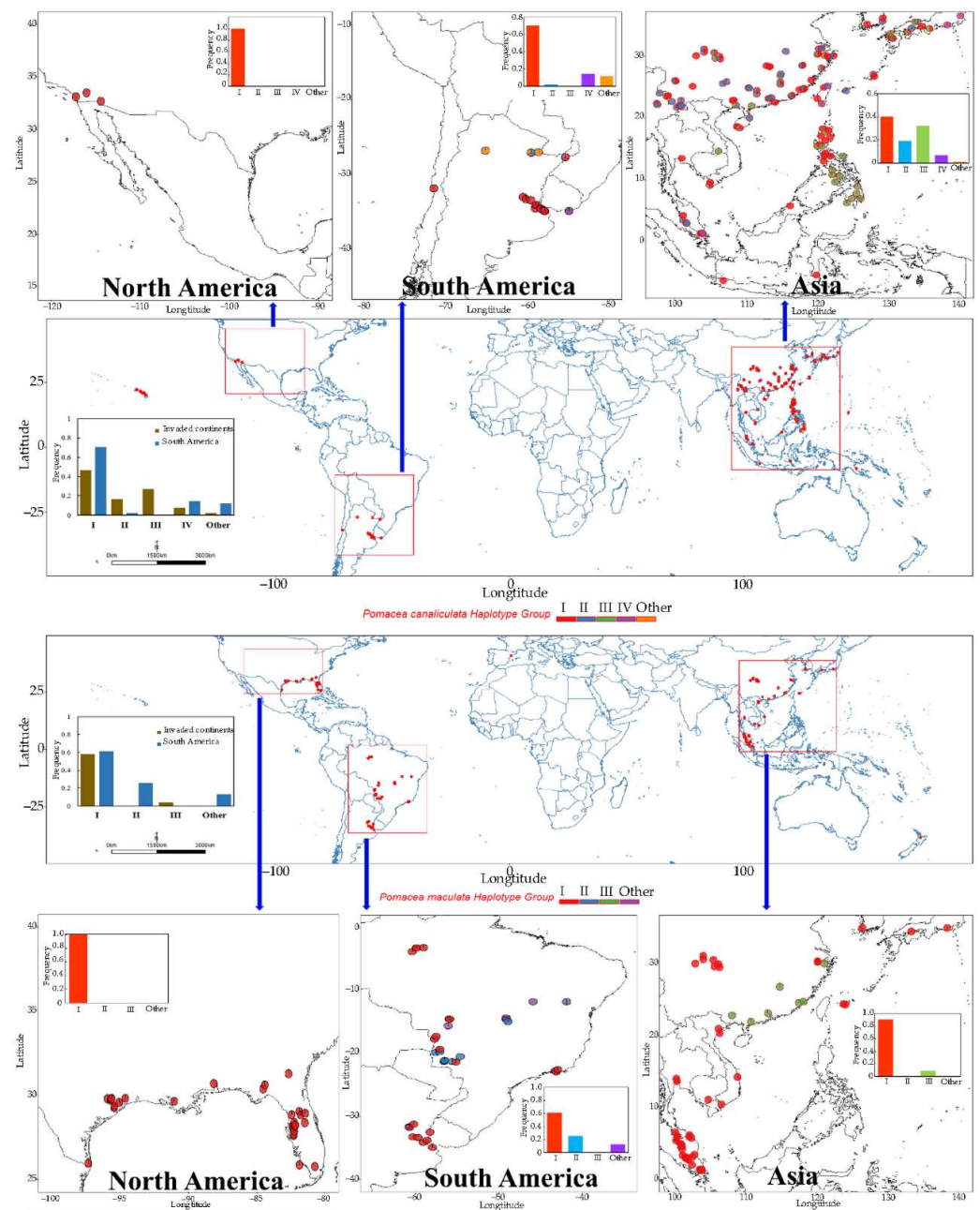


**Figure 4.** Haplotype networks distribution of *Pomacea canaliculata* and *Pomacea maculata* in invaded continents and South America.

According to the RDA analysis results, the first two axes explained over 80% of the variation in the haplotype distribution of *P. canaliculata* and *P. maculata* due to climate factors (Figure 5). Pc6 was related to 'Precipitation (Mar–May, mm)', whereas Pc3 was tied to 'Altitude above sea level'. Other *P. canaliculata* haplotypes were all related to five climate factors. Pm1 was subjected to 'Precipitation (Sep–Nov)' and 'Days of avg. temp.  $\geq 35\text{ }^{\circ}\text{C}$ '. Most *P. maculata* haplotypes were closely related to 'Days of max. temp.  $\geq 35\text{ }^{\circ}\text{C}$ ', 'Precipitation (Mar–May)', and 'Altitude above sea level'. The *P. canaliculata* haplotypes in Asia were related to all five factors, while those in South America were related to 'Days of avg. temp.  $\geq 18\text{ }^{\circ}\text{C}$ ' and 'Extreme lowest temp.', possibly due to the lower influence of human activity on food in the native range. The *P. maculata* haplotypes in Asia and Oceania were both closely related to 'Days of avg. temp.  $\geq 35\text{ }^{\circ}\text{C}$ ' and 'Extreme lowest temp.', whereas those in South America were tied to 'Days of max. temp.  $\geq 35\text{ }^{\circ}\text{C}$ ' and 'Precipitation (Mar–May)'.

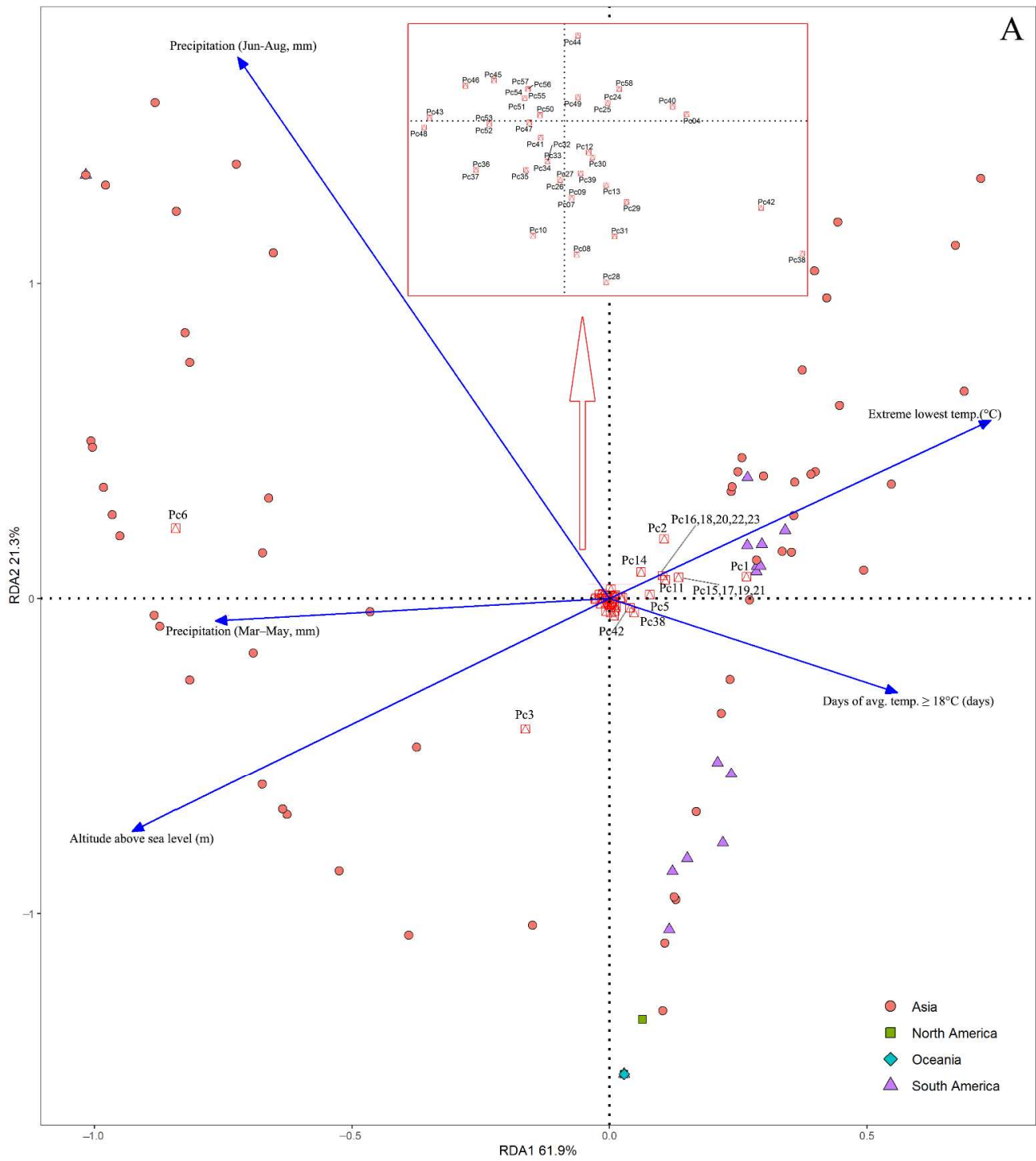
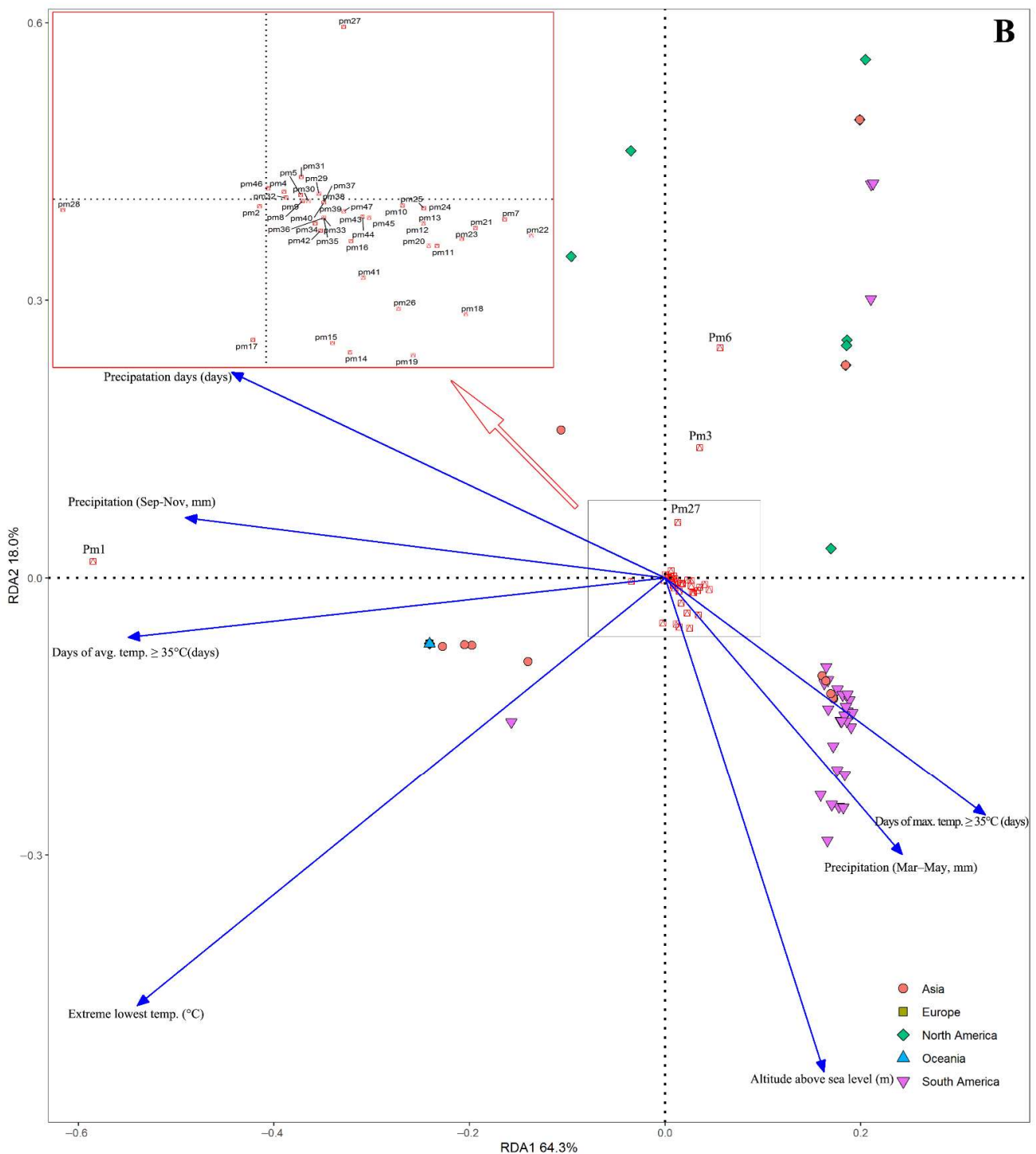


Figure 5. Cont.



**Figure 5.** Redundancy analysis between haplotypes of *Pomacea canaliculata* ((A), Pc1 to 58) and *Pomacea maculata* ((B), Pm1 to 47) of continental populations and climate factors.

### 3.4. Genetic Structure and Isolation by Distance of *P. canaliculata* and *P. maculata*

Significant genetic differentiation existed between populations in the invaded and native areas (Table 4). At the continental level, the overall  $\Phi_{ST}$ ,  $\Phi_{SC}$  and  $\Phi_{CT}$  of the *P. canaliculata* populations were 0.3339, 0.1262, and 0.2377. Molecular variance among continents was significant and accounted for 23.77% of the total variation ( $\Phi_{CT} = 0.2377$ ), indicating a possible structure partitioning of the *P. canaliculata* populations in the continents. The majority of the hierarchical molecular variance accounted for 66.61% within population comparisons. Significant genetic differentiation of the *P. maculata* populations was ob-

served among populations within the continents and within the populations ( $p < 0.01$ ). The overall  $\Phi_{ST}$ ,  $\Phi_{SC}$ , and  $\Phi_{CT}$  of the *P. maculata* populations were 0.3802, 0.1920, and 0.2329, respectively. The AMOVA indicated that the genetic differentiation among continents of the *P. maculata* populations contributed 23.29% to the total variation.

**Table 4.** Analysis of molecular variance (AMOVA) for COI in *Pomacea canaliculata* and *Pomacea maculata* populations.

Speices	Source of Variation	df	Sum of Squares	Variance Components	Percentage of Variation	<i>p</i>	Fixation Indices
<i>P. canaliculata</i>	Among continents	3	444.638	2.8366	23.77	0.0039	$\Phi_{CT} = 0.2377$
	Among populations within continent	14	283.344	1.1483	9.62	0.0000	$\Phi_{SC} = 0.1262$
	Within populations	712	5660.489	7.9501	66.61	0.0000	$\Phi_{ST} = 0.3339$
	Total	729	6383.471	11.9350			
<i>P. maculata</i>	Among continents	4	403.554	1.7008	23.29	0.0890	$\Phi_{CT} = 0.2329$
	Among populations within continent	8	121.715	1.0758	14.73	0.0020	$\Phi_{SC} = 0.1920$
	Within populations	219	991.318	4.5266	61.98	0.0000	$\Phi_{ST} = 0.3802$
	Total	231	1516.587	7.3032			

The overall  $F_{ST}$  value of *P. canaliculata* and *P. maculata* between the invaded and native areas was 0.2657 ( $p = 0.000$ ) and 0.3097 ( $p = 0.000$ ). The  $F_{ST}$  values among continental populations of *P. canaliculata* and *P. maculata* ranged respectively from 0 to 0.3663 and from 0 to 0.5810 (Supplementary Materials Figure S5A). Significant pairwise  $F_{ST}$  values existed among the *P. canaliculata* populations of Asia, North America, and South America. Except for Oceania, significant pairwise  $F_{ST}$  values of the *P. maculata* population were observed between South America and the invaded continents. A highly significant  $F_{ST}$  value appeared between the *P. canaliculata* populations (Asia vs. North America, 0.3663) and *P. maculata* populations (Europe vs. North America, 0.5810). The gene flow among continental populations of *P. canaliculata* and *P. maculata* respectively ranged from 0.8650 to 4.1512 and from 0.3606 to 1.4506 (Supplementary Materials Figure S5B).

Isolation-by-distance (IBD) analysis was performed in populations of the invaded continents, Asia, and South America (Figure 6). The Mantel test verified a highly significant correlation ( $p = 0.001$ ) between the Nei genetic distance and geographical distances among *P. canaliculata* in the invaded continents ( $r = 0.060$ ), Asia ( $r = 0.129$ ), and the native area ( $r = 0.525$ ). A significant correlation ( $p = 0.001$ ) also existed among *P. maculata* in the invaded continents ( $r = 0.316$ ), Asia ( $r = 0.350$ ), and the native area ( $r = 0.216$ ).

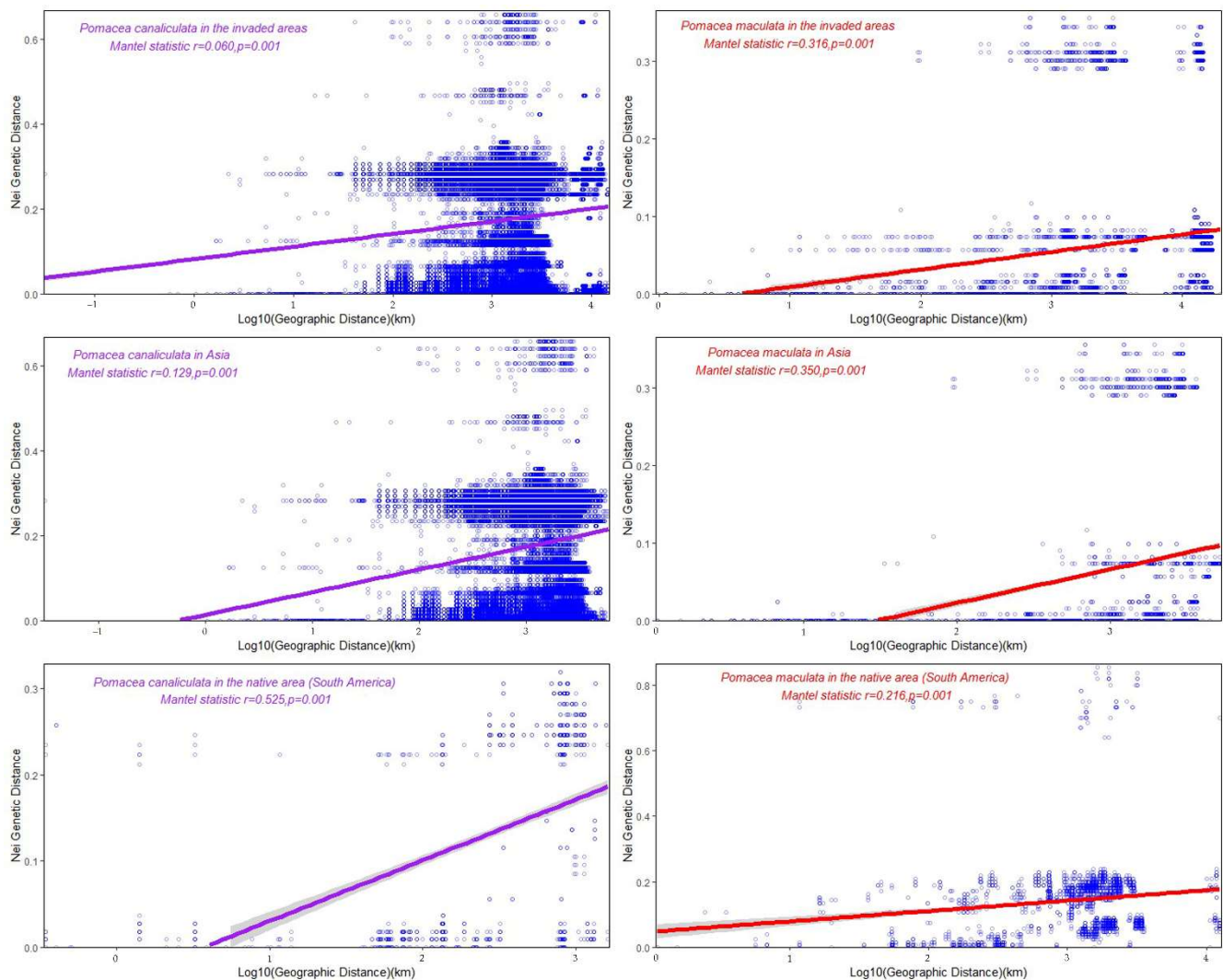


**Figure 6.** Analysis of Isolation-by-Distance between geographic distance and Nei distance of *P. canaliculata* and *P. maculata* populations in invaded continents, Asia and South America.

## 4. Discussion

### 4.1. Genetic Diversity and Population History

The haplotype diversity and nucleotide diversity are two essential indexes for measuring genetic diversity [54]. The relatively high haplotype diversity coupled with the low nucleotide diversity in *P. maculata* may be due to the relatively large population size and small differences between sequences. This phenomenon was also possibly the result of the initial multiple introductions of *P. maculata* [12], which subsequently suffered from a bottleneck effect from climate factors and agricultural activity. The snail *Humboldtiana durangoensis* population also showed a high haplotype diversity and a low nucleotide diversity during expansion [55]. Rapid population expansion helps accumulate haplotype diversity, while the accumulation of nucleotide polymorphisms is hard for a limited time [56].

Compared with natural habitats, agricultural habitats were partly isolated habitats that are frequently disturbed by routine management, including pesticide application, fertilization, plowing, and drainage. Agricultural management strategies, especially molluscicide application, have dramatically affected the population dynamics of apple snails and alleviated the harm to rice production [7]. The diverse perturbation in agricultural habitat led to the loss of nucleotide variation and an even distribution of *P. canaliculata* haplotypes, which explains the lower nucleotide diversity and higher haplotype diversity in the *P. canaliculata* populations from agricultural habitats compared with natural habitats.

Unexpectedly, the nucleotide variation in the COI gene of the *P. maculata* population and the proportion of some haplotypes were higher in the agricultural habitat compared with the non-agricultural habitat, leading to the opposite changes in the nucleotide diversity and the haplotype diversity. Considering the relatively high haplotype diversity and low nucleotide diversity, *P. canaliculata* and *P. maculata* experienced the ‘bottleneck effect’ and ‘founder effect’ in the agricultural habitat [57]. This study demonstrated a correlation between genetic diversity at a single locus and habitat differentiation. However, a pattern in diversity changes can be influenced by numerous factors in the natural environment and more researches is needed. As the introductions of the two snails in the invaded areas gradually stopped due to the strict regulation, the two snails developed a differential response to agricultural management at the genetic level based on the initial gene pool.

Different sensitivities of  $F_u$ 's  $F_s$  and SSD in testing the population expansion of the two invasive snails were observed as the expansion may have been restricted in separated areas, which led to non-significant  $F_u$ 's  $F_s$  values [54]. This discrepancy in detecting population expansion can be interpreted as a reduction, a subdivision, a bottleneck, or migration of the population [54,58]. Demographic expansion followed by a bottleneck possibly occurred in the *P. maculata* populations in the invaded continents, partly explaining a multimodal pattern of population differentiation. The populations of the two invasive snails acted differently under selection during the successful establishment. The differentiation in physiological responses of *P. canaliculata* and *P. maculata* to cold, salinity, pH, and desiccation was possibly involved in invasion patterns [19,33].

#### 4.2. Haplotype Network and Its Relation to Climate Factors

The founder effect can lead to a low genetic variability and a limited genetic pool of snail populations [59]. Previous studies reported many *P. canaliculata* haplotypes in Asia [7,15]. Similarly, our analysis also showed that the number of haplotype types in *P. canaliculata* populations from the invaded continents was high compared with that from the native area. The colonization of *P. canaliculata* in the invaded continents was not entirely restricted by the founder effect due to the admixed invasion or multiple introductions [7,15]. We speculated that seven new *P. canaliculata* haplotypes discovered in this study might be due to the potential introduction process or increased samplings. Furthermore, the new haplotypes of Pc56 showed a vital connection between Network III and Network I. Another possibility is that the sampling in South America was insufficient to identify Network III and further sampling would help in a clear elaboration.

We found two haplotypes of *P. maculata* that were not shared with other continents which have been invaded by *P. maculata*. The locations (Nanning, Zhangzhou, China) of the new *P. maculata* haplotype were up to 1500 km away from the reported locations in Sichuan, Chongqing, and Zhejiang Provinces [15]. Meanwhile, in a recent survey of *P. maculata* populations in Thailand, six new haplotypes from 27 obtained COI sequences of *P. maculata* were identified, which were not shared with those in the native areas, despite the widely distributed situation in Thailand [60]. We concluded that insufficient samplings were possibly common in Asia, and that the new haplotypes of *P. maculata* were originated from previously non-sampled locations.

RDA analysis showed that the climate factors were closely related to haplotypes. The individuals may have been adapted to the climate factors before or after introduction. The haplotypes (Pc6, Pc3, and Pm1) were closely tied to precipitation, altitude and temperature. Generally, the precipitation and temperature distribution changed due to the altitude variation. Thus, the precipitation and temperature were important for haplotypes in the invaded continents and South America. Haplotype Pc6 was discovered only in the invaded continents and was significantly related to precipitation from March to May. Most of the Pc6 haplotypes existed in individuals sampled in South China. This is consistent with the phenomenon of the establishment of *P. canaliculata* populations in paddy fields, as the rainy season and rice-planting season normally start in March in South China.

#### 4.3. Genetic Differentiation and Isolation by Distance

IBD is used to explain the genetic variation in snail populations [61]. The genetic differentiation of *P. canaliculata* between the invaded continents and the native area based on AMOVA was consistent with the assumption that IBD increases the genetic dissimilarity between populations. The geographic barriers also negatively influenced the gene exchange of *P. canaliculata* or *P. maculata* between continents.

The seven new sequences of *P. canaliculata* came from three sampling locations (Nanning, Nankang, Shifang, China) that were unconnected to each other in China, and the minimum distance between the three locations exceeds 700 km. These new haplotypes appearing in three remote sampling sites suggested that potential haplotypes existed in China. These sequences possibly came from multiple introductions of *P. canaliculata* or from the unsampled individuals in China.

## 5. Conclusions

Apple snails have invaded numerous areas with frequent human interference since the first introduction from South America. We studied the genetic diversity, haplotype distribution and population differentiation of the two invasive apple snails, and may conclude that (1) agricultural measures have influenced the genetic diversity of the two invasive snails; (2) the two invasive snails have been acclimated to the climate factors; and (3) the two morphologically similar snails show differential genetic patterns in the invaded continents concerning the population history and the number and structure of haplotype networks. Performing a comprehensive global analysis, including molecular data and morphological data, is necessary in future work, which will also help in the understanding of the management effect against *P. canaliculata* and *P. maculata*.

**Supplementary Materials:** The following supporting information can be downloaded at: <https://www.mdpi.com/article/10.3390/d14121069/s1>, Figure S1: Location of climate stations used in this study; Figure S2: Climate information (temperature) used in this study; Figure S3: Climate information (precipitation and altitude) used in this study; Figure S4: Mismatch distribution of *P. canaliculata* and *P. maculata* in invaded continents and South America; Figure S5: Pairwise genetic differentiation index (FST) (A) and gene flow (B) of *Pomacea canaliculata* and *Pomacea maculata* in continents. \* Significant level at  $p < 0.05$  (values in red font); Table S1: The sampling locations of apple snail populations in South China; Table S2: Climate information of *Pomacea canaliculata* and *Pomacea maculata* sequences; Table S3: Sequence information of *Pomacea canaliculata* and *Pomacea maculata*; Table S4: Habitat information of *Pomacea canaliculata* and *Pomacea maculata* sequences; Table S5: Sequences traits of *Pomacea canaliculata* and *Pomacea maculata*; Table S6: Haplotypes of *Pomacea canaliculata* and *Pomacea maculata* in continents

**Author Contributions:** Conceptualization, B.Z. and J.Z.; Formal analysis, B.Z.; Funding acquisition, J.Z.; Investigation, B.Z., M.L., Y.L., Z.D. and X.G.; Project administration, J.Z.; Resources, M.L., Y.L., Z.D. and X.G.; Writing—original draft, B.Z.; Writing—review and editing, J.Z. All authors have read and agreed to the published version of the manuscript.

**Funding:** This work was funded by National Natural Science Foundation of China (31870525, 31770484, U1131006 and 41871034), Science and Technology Planning Project of Guangdong Province of China (2019B030301007) and Undergraduate Innovation Programs (201713050216).

**Institutional Review Board Statement:** Not applicable.

**Data Availability Statement:** The data presented in this study are available in Supplementary Materials.

**Acknowledgments:** The authors thank undergraduates and postgraduates in the Guangdong Provincial Key laboratory of Eco-Circular Agriculture, South China Agricultural University for the assistance with samples collection.

**Conflicts of Interest:** The authors declare no conflict of interest.

## References

1. Sherpa, S.; Despres, L. The evolutionary dynamics of biological invasions: A multi-approach perspective. *Evol. Appl.* **2021**, *14*, 1463–1484. [[CrossRef](#)] [[PubMed](#)]
2. Hofstadter, D.F.; Kryshak, N.F.; Wood, C.M.; Dotters, B.P.; Roberts, K.N.; Kelly, K.G.; Keane, J.J.; Sawyer, S.C.; Shaklee, P.A.; Kramer, H.A.; et al. Arresting the spread of invasive species in continental systems. *Front. Ecol. Environ.* **2022**, *20*, 278–284. [[CrossRef](#)]
3. Yarra, A.N.; Magoulick, D.D. Modelling effects of invasive species and drought on crayfish extinction risk and population dynamics. *Aquat. Conserv.* **2019**, *29*, 1–11. [[CrossRef](#)]
4. Kotov, A.A.; Karabanov, D.P.; Van Damme, K. Non-indigenous Cladocera (Crustacea: Branchiopoda): From a few notorious cases to a potential global faunal mixing in aquatic ecosystems. *Water* **2022**, *14*, 2806. [[CrossRef](#)]
5. Azmi, W.A.; Khoo, S.C.; Ng, L.C.; Baharuddin, N.; Aziz, A.A.; Ma, N.L. The current trend in biological control approaches in the mitigation of golden apple snail *Pomacea* spp. *Biol. Control.* **2022**, *175*, 105060. [[CrossRef](#)]
6. Naylor, R. Invasions in agriculture: Assessing the cost of the golden apple snail in Asia. *Ambio* **1996**, *25*, 443–448.
7. Horgan, F.G. Ecology and management of apple snails in rice. In *Rice Production Worldwide*; Chauhan, B., Jabran, K., Mahajan, G., Eds.; Springer: Cham, Switzerland, 2017.
8. Lowe, S.; Browne, M.; Boudjelas, S.; De Poorter, M. *100 of the World's Worst Invasive Alien Species: A Selection from the Global Invasive Species Database*; Invasive Species Specialist Group: Auckland, New Zealand, 2000.
9. Horgan, F.G.; Stuart, A.M.; Kudavidanage, E.P. Impact of invasive apple snails on the functioning and services of natural and managed wetlands. *Acta Oecol.* **2014**, *54*, 90–100. [[CrossRef](#)]
10. Gilioli, G.; Schrader, G.; Carlsson, N.; van Donk, E.; van Leeuwen, C.H.A.; Martín, P.R.; Pasquali, S.; Vilà, M.; Vosi, S. Environmental risk assessment for invasive alien species: A case study of apple snails affecting ecosystem services in Europe. *Environ. Impact. Asses.* **2017**, *65*, 1–11. [[CrossRef](#)]
11. Xu, Y.X.; Wang, W.S.; Yao, J.M.; Yang, M.L.; Guo, Y.H.; Deng, Z.H.; Mao, Q.; Li, S.Z.; Duan, L.P. Comparative proteomics suggests the mode of action of a novel molluscicide against the invasive apple snail *Pomacea canaliculata*, intermediate host of *Angiostrongylus cantonensis*. *Mol. Biochem. Parasit.* **2022**, *247*, 111431. [[CrossRef](#)]
12. Hayes, K.A.; Joshi, R.C.; Thiengo, S.C.; Cowie, R.H. Out of South America: Multiple origins of non-native apple snails in Asia. *Divers. Distrib.* **2008**, *14*, 701–712. [[CrossRef](#)]
13. Rao, S.R.; Liew, T.S.; Yow, Y.Y.; Ratnayeke, S. Cryptic diversity: Two morphologically similar species of invasive apple snail in Peninsular Malaysia. *PLoS ONE* **2018**, *13*, e0196582.
14. Luo, M.Z.; Zhao, B.L.; Zhang, J.E.; Qin, Z. Phenotypic plasticity of the invasive apple snail, *Pomacea canaliculata*, in China: A morphological differentiation analysis. *Molluscan Res.* **2022**, *42*, 146–157. [[CrossRef](#)]
15. Yang, Q.Q.; Liu, S.W.; He, C.; Yu, X.P. Distribution and the origin of invasive apple snails, *Pomacea canaliculata* and *P. maculata* (Gastropoda: Ampullariidae) in China. *Sci. Rep.* **2018**, *8*, 1–8. [[CrossRef](#)] [[PubMed](#)]
16. Andree, K.B.; López, M.A. Species identification from archived snail shells via genetic analysis: A method for DNA extraction from empty shells. *Molluscan Res.* **2013**, *33*, 1–5. [[CrossRef](#)]
17. Yang, Q.Q.; Yu, X.P. A new species of apple snail in the genus *Pomacea* (Gastropoda: Caenogastropoda: Ampullariidae). *Zool. Stud.* **2019**, *58*, 13.
18. Litsinger, J.A.; Estano, D.B. Management of the golden apple snail *Pomacea canaliculata* (Lamarck) in rice. *Crop. Prot.* **1993**, *12*, 363–370. [[CrossRef](#)]
19. Yoshida, K.; Wada, T.; Matsukura, K.; Shiba, T. Potential overwintering areas of the alien apple snail, *Pomacea canaliculata*, in Japan at its northern distribution limit. *Aquat. Invasions* **2022**, *17*, 402–414. [[CrossRef](#)]
20. Matsukura, K.; Izumi, Y.; Yoshida, K.; Wada, T. Cold tolerance of invasive freshwater snails, *Pomacea canaliculata*, *P. maculata*, and their hybrids helps explain their different distributions. *Freshw. Biol.* **2016**, *61*, 80–87. [[CrossRef](#)]
21. State Environmental Protection Administration and Chinese Academy of Sciences. Circular on Publishing the List of the First Batch of Alien Invasive Species in China. 2003. Available online: [https://www.gov.cn/gongbao/content/2003/content\\_62285.htm](https://www.gov.cn/gongbao/content/2003/content_62285.htm) (accessed on 18 October 2022).
22. Rawlings, T.A.; Haye, K.A.; Cowie, R.H.; Collins, T.M. The identity, distribution, and impacts of non-native apple snails in the continental united states. *BMC Evol. Biol.* **2007**, *7*, 97. [[CrossRef](#)]
23. Yang, Q.Q.; Liu, S.W.; He, C.; Cowie, R.H.; Yu, X.P.; Hayes, K.A. Invisible apple snail invasions: Importance of continued vigilance and rigorous taxonomic assessments. *Pest. Manag. Sci.* **2019**, *75*, 1277–1286. [[CrossRef](#)]
24. Folmer, O.; Black, M.; Hoeh, W.; Lutz, R.; Vrijenhoek, R. DNA primers for amplification of mitochondrial cytochrome c oxidase subunit I from diverse metazoan invertebrates. *Mol. Mar. Biol. Biotech.* **1994**, *3*, 294–299.
25. Hall, T.A. BioEdit: A user-friendly biological sequence alignment editor and analysis program for Windows 95/98/NT. *Nucleic Acids Symp. Ser.* **1999**, *41*, 95–98.
26. Matsukura, K.; Okuda, M.; Kubota, K.; Wada, T. Genetic divergence of the genus *Pomacea* (Gastropoda: Ampullariidae) distributed in Japan, and a simple molecular method to distinguish *P. canaliculata* and *P. insularum*. *Appl. Entomol. Zool.* **2008**, *43*, 535–540. [[CrossRef](#)]
27. Hayes, K.A.; Cowie, R.H.; Thiengo, S.C. A global phylogeny of apple snails: Gondwanan origin, generic relationships, and the influence of outgroup choice (Caenogastropoda: Ampullariidae). *Biol. J. Linn. Soc.* **2009**, *98*, 61–76. [[CrossRef](#)]

28. Song, H.M.; Hu, Y.C.; Wang, P.X.; Mou, X.D.; Li, X.H.; Wang, X.J.; Luo, J.R. Sequencing cytochrome oxidase subunit I of mitochondrial DNA and the taxonomic status of apple snails. *Chin. J. Zool.* **2010**, *45*, 1–7.
29. Collier, K.J.; Demetras, N.J.; Duggan, I.C.; Johnston, T.M. Wild record of an apple snail in the Waikato river, Hamilton, New Zealand, and their incidence in freshwater aquaria. *New Zealand Nat. Sci.* **2011**, *36*, 1–9.
30. Martin, C.W.; Baya, K.M.; Valentine, J.F. Establishment of the invasive island apple snail *Pomacea insularum* (gastropoda: Ampullariidae) and eradication efforts in mobile, Alabama, USA. *Gulf Mex. Sci.* **2012**, *56*, 30–38. [[CrossRef](#)]
31. Matsukura, K.; Okuda, M.; Cazzaniga, N.J.; Wada, T. Genetic exchange between two freshwater apple snails, *Pomacea canaliculata* and *Pomacea maculata* invading east and southeast Asia. *Biol. Invasions* **2013**, *15*, 2039–2048. [[CrossRef](#)]
32. Mu, H.; Sun, J.; Fang, L.; Luan, T.; Williams, G.A.; Cheung, S.G. Genetic basis of differential heat resistance between two species of congeneric freshwater snails: Insights from quantitative proteomics and base substitution rate analysis. *J. Proteome Res.* **2015**, *14*, 4296–4308. [[CrossRef](#)]
33. Deaton, L.E.; Schmidt, W.; Leblanc, B.; Carter, J.; Mueck, K.; Merino, S. Physiology of the invasive apple snail *Pomacea maculata*: Tolerance to low temperatures. *J. Shellfish Res.* **2016**, *35*, 207–210. [[CrossRef](#)]
34. Letelier, S.; Rebolledo, A.; Báez, P.; Fabres, A.; Soto-Acuña, S.; Jackson, D. The highly invasive freshwater apple snail *Pomacea canaliculata* (Gastropoda: Ampullariidae) in northern Chile: Morphological and molecular confirmation. *J. Zool. Stud.* **2016**, *3*, 119–128.
35. Yang, Q.Q.; Liu, S.W.; Ru, W.D.; Liu, G.F.; Yu, X.P. Molecular identification of invasive golden apple snails in Zhejiang Province based on DNA barcoding. *Biodivers. Sci.* **2016**, *24*, 341–350. (In Chinese)
36. Boclaer, B.V.; Strong, E.E.; Richter, R.; Stelbrink, B.; Rintelen, T.V. Anatomical and genetic data reveal that *rivularia heude*, 1890 belongs to Viviparinae (Gastropoda: Viviparidae). *Zool. J. Linn. Soc. Lond.* **2017**, *182*, 1–23. [[CrossRef](#)]
37. Perez, K.E.; Gamboa, V.G.; Schneider, C.M.; Burks, R.L. Resaca supports range expansion of invasive apple snails (*Pomacea maculata* perry, 1810; Caenogastropoda: Ampullariidae) to the Rio Grande Valley, Texas. *Check List* **2017**, *13*, 2134. [[CrossRef](#)]
38. Zhang, C.L.; Peng, J.; Ran, Z.; Zi, J.R.; Yang, Y.M. Genotyping and polymorphism analysis of cytochrome c oxidase subunit I gene of *Pomacea canaliculata* from Lincang City in Yunnan Province. *Chin. J. Schisto. Control* **2018**, *30*, 179–183. (In Chinese)
39. Ng, T.H.; Tan, S.K.; Ahmad, A.; Joshi, R.C.; Wang, W.Y.; Tan, H.H. Not in the Least Concern: Anthropogenic influences on a South-east Asian apple snail *Pila scutata* (Ampullariidae). *Oryx* **2019**, *53*, 230–238. [[CrossRef](#)]
40. Zhang, C.L.; Bao, X.Y.; Peng, J.; Zi, J.R.; Ran, Z.; Lu, N.; Yang, Y.M. Species identification of *Pomacea* snails in southwest Yunnan Province based on COI gene polymorphism. *Chin. J. Parasitol. Parasit. Dis.* **2019**, *37*, 75–86. (In Chinese)
41. Edgar, R.C. MUSCLE: Multiple sequence alignment with high accuracy and high throughput. *Nucleic Acids Res.* **2004**, *32*, 1792–1797. [[CrossRef](#)]
42. Kumar, S.; Stecher, G.; Li, M.; Nnyaz, C.; Tamura, K. MEGA X: Molecular evolutionary genetics analysis across computing platforms. *Mol. Biol. Evol.* **2018**, *35*, 1547–1549. [[CrossRef](#)]
43. Librado, P.; Rozas, J. DnaSP v5: A software for comprehensive analysis of DNA polymorphism data. *Bioinformatics* **2009**, *25*, 1451–1452. [[CrossRef](#)]
44. Excoffier, L.; Laval, G.; Schneider, S. Arlequin ver. 3.0: An integrated software package for population genetics data analysis. *Evol. Bioinform.* **2005**, *1*, 47–50. [[CrossRef](#)]
45. R Core Team. R: A Language and Environment for Statistical Computing R Foundation for STATISTICAL Computing, Vienna, Austria. 2020. Available online: <https://www.R-project.org/> (accessed on 18 October 2022).
46. Paradis, E. Pegas: An R package for population genetics with an integrated-modular approach. *Bioinformatics* **2010**, *26*, 419–420. [[CrossRef](#)] [[PubMed](#)]
47. Leigh, J.W.; Bryant, D. POPART: Full-feature software for haplotype network construction. *Methods Ecol. Evol.* **2015**, *6*, 1110–1116. [[CrossRef](#)]
48. Wickham, H. *Ggplot2: Elegant Graphics for Data Analysis*, 2nd ed.; Springer-Verlag: New York, NY, USA, 2018.
49. Bivand, R. The Maptool Package Version. 2019, 0.9-5. Available online: <https://cran.r-project.org/src/contrib/Archive/maptools> (accessed on 18 October 2022).
50. Yu, G.C. The Scatterpie Package Version 0.1.2.2019. Available online: <https://cran.r-project.org/web/packages/scatterpie/index.html> (accessed on 18 October 2022).
51. Oksanen, J.; Blanchet, F.G.; Friendly, M.; Kindt, R.; Legendre, P.; McGlinn, D.; Minchin, P.R.; O’Hara, R.B.; Simpson, G.L.; Solymos, P.; et al. Vegan: Community Ecology Package. R Package Version 2.5-6. 2019. Available online: <https://CRAN.R-project.org/src/contrib/Archive/vegan> (accessed on 18 October 2022).
52. Slowikowski, K. Ggrepel: Automatically Position Non-Overlapping Text Labels with ‘Ggplot2’ R Package Version 0.8.2. 2020. Available online: <https://CRAN.R-project.org/src/contrib/Archive/ggrepel> (accessed on 18 October 2022).
53. Lefort, V.; Longueville, J.E.; Gascuel, O. SMS: Smart Model Selection in PhyML. *Mol. Biol. Evol.* **2017**, *34*, 2422–2424. [[CrossRef](#)] [[PubMed](#)]
54. Liao, P.C.; Kuo, D.C.; Lin, C.C.; Ho, K.C.; Lin, T.P.; Hwang, S.Y. Historical spatial range expansion and a very recent bottleneck of *Cinnamomum kanehirae* Hay. (Lauraceae) in Taiwan inferred from nuclear genes. *BMC Evol. Biol.* **2010**, *10*, 124. [[CrossRef](#)]
55. López, B.; Zúñiga, G.; Mejiá, O. Phylogeographic structure in the apparent absence of barriers: A case study of the Mexican land snail *Humboldtiana durangoensis* (Pulmonata: Humboldtianidae). *J. Molluscan Stud.* **2019**, *85*, 244–252. [[CrossRef](#)]

56. Zhang, Q.; Sun, C.; Zhu, Y.; Xu, N.; Liu, H. Genetic diversity and structure of the round-tailed paradise fish (*Macropodus ocellatus*): Implications for population management. *Glob. Ecol. Conserv.* **2020**, *21*, e00876. [[CrossRef](#)]
57. Arekar, K.; Tiwari, N.; Sathyakumar, S.; Khaleel, M.; Karanth, P. Geography vs. past climate: The drivers of population genetic structure of the Himalayan langur. *BMC Ecol. Evo.* **2022**, *22*, 100. [[CrossRef](#)]
58. Wang, Q.Q.; Shaheen, T.; Rong, L.; Tang, G.H. Phylogeography of walnut pest *Atrijuglans hetaohei* (Lepidoptera: Gelechioidea) reveals comprehensive influence of geographic barriers and human activities. *J. Asia-Pac. Entomol.* **2022**, *25*, 101962.
59. Nehemia, A.; Ngendu, Y.; Kochzius, M. Genetic population structure of the mangrove snails *Littoraria subvittata* and *L. pallescens* in the Western Indian Ocean. *J. Exp. Mar. Bio. Ecol.* **2019**, *514*, 27–33. [[CrossRef](#)]
60. Dumida, A.; Janthu, P.; Subkrasae, C.; Polseela, R.; Mangkit, B.; Thanwisai, A.; Vitta, A. 2021. Population genetics analysis of a Pomacea snail (Gastropoda: Ampullariidae) in Thailand and its low infection by *Angiostrongylus cantonensis*. *Zool. Stud.* **2021**, *60*, 31.
61. Valladares, M.A.; Fabres, A.A.; Collado, G.A.; Saez, P.A.; Mendez, M.A. Coping with dynamism: Phylogenetics and phylogeographic analyses reveal cryptic diversity in *heleobia* snails of Atacama Saltpan, Chile. *Front. Ecol. Evol.* **2022**, *10*, 869626. [[CrossRef](#)]